Shot-noise suppression in resonant tunneling

H. C. Liu,* Jianmeng Li, G. C. Aers, C. R. Leavens, M. Buchanan, and Z. R. Wasilewski
Institute for Microstructural Sciences, National Research Council, Ottawa, Ontario, Canada K1A 0R6
(Received 22 September 1994)

Substantial shot-noise suppression has been observed in a series of asymmetric double-barrier resonant-tunneling diodes. The suppression is only seen in the voltage range where the peak resonant-tunneling transmission coefficient is near unity and where there is a large charge buildup in the quantum well; in other voltage ranges, full shot noise is observed.

Since the first experimental demonstration,[1] resonant tunneling has been one of the most interesting phenomena in semiconductor heterostructures and has found some unique high-frequency applications.[2,3] Although the basic physics is now well understood, resonant tunneling continues to serve as a unique tool to study electron transport in nanostructures.[4,5] Recently, the noise associated with electron transport in nanostructures has attracted a lot of theoretical attention.[6–10] The study of noise in nanostructures is both interesting from a pure physics point of view and important for future device applications. There have been three previous reports[10–12] on experimental results of noise characteristics in resonant-tunneling diodes showing shot-noise suppression, i.e., $\gamma < 1$ for $i_n^2 = 2e\gamma I$, where i_n is the measured noise current in $A/Hz^{1/2}$, I is the device current, and γ is referred to as the shot-noise factor. The case $\gamma = 1$ corresponds to full shot noise. In this paper, we report on the results of a study of a series of three resonant-tunneling diodes designed to maximize shot-noise suppression. Simple analytical models are considered and comparisons with self-consistent model calculations are also presented.

We first present the experimental results. The resonant-tunneling structures were grown by $GaAs/Al_xGa_{1-x}As$ molecular beam epitaxy with Si doping. All samples were made intentionally asymmetric. The active layer parameters of the three samples are given in Table I. Undoped GaAs spacer layers of 5.0 nm were grown on either side of the active layers, and these layers were clad with thick contact layers of GaAs doped with Si to 2×10^{18} cm^{-3}. The asymmetry was in either the barrier thickness or the barrier height: samples 1 and 2 had one barrier thicker than the other ($L_{b2} > L_{b1}$), while sample 3 had one barrier higher than the other ($x_2 > x_1$). Measurements were done at 77 and 4.2 K with samples immersed in liquid nitrogen or helium. Measured device current vs voltage and noise current vs voltage at 4.2 K are shown in Fig. 1 and similar results were observed at 77 K. Positive bias polarity is defined such that electrons are emitted from the thin or low barrier side. The diode active area diameters were 7 μm. The noise was measured at low frequencies for the device but high enough to avoid $1/f$ noise contributions, typically at

TABLE I. Sample parameters. All wells are undoped GaAs, and all barriers are undoped $Al_xGa_{1-x}As$. The symbols L_{b1}, x_1, L_w, L_{b2}, and x_2 are the first barrier width, the first barrier Al fraction, the well width, the second barrier width, and the second barrier Al fraction, respectively.

Sample	L_{b1} (nm)	x_1	L_w (nm)	L_{b2} (nm)	x_2
1	9.5	0.37	5.9	13.3	0.37
2	10.0	0.33	6.6	14.0	0.33
3	10.0	0.33	5.6	10.0	0.50

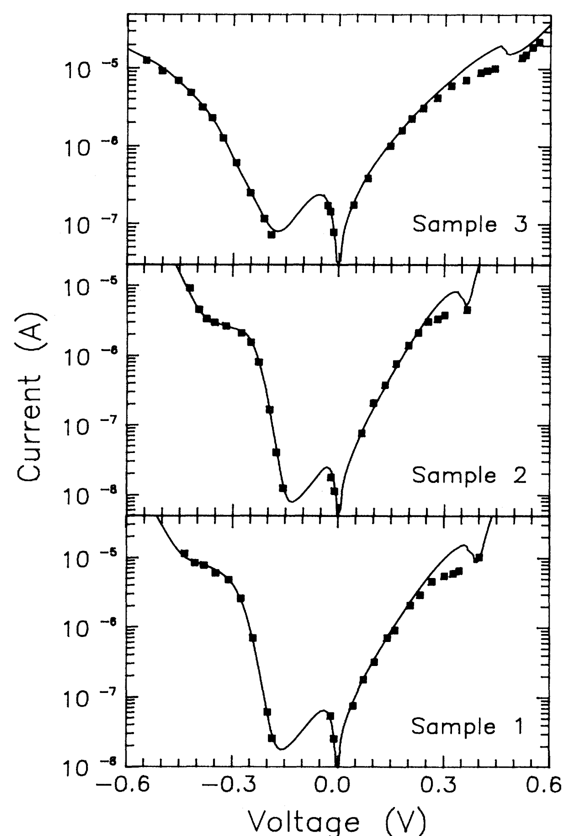

FIG. 1. Measured current (solid lines) and noise current (symbols) vs voltage at 4.2 K. Positive bias corresponds to electrons emitted from the thinner or lower barrier side. To plot the noise current on the same scale as that for the current, the quantity $i_n^2/2e$ is plotted, where i_n is the noise current in $A/Hz^{1/2}$. The device active area diameters were 7 μm.

frequencies above 1 kHz. The frequency regime studied here is much lower than the reciprocal of any resonant-tunneling characteristic times involved in our devices, so that we are in effect dealing with the device shot noise in the zero-frequency limit. We stress that our wafers and devices made from the same wafer were very uniform, and the results shown in Fig. 1 are representative of the three wafers. Our standard procedure is that a piece of about 7×8 mm^2 is cleaved from each wafer, and an array of a large number of devices is made. No further investigation is pursued *unless* these devices display the *same* characteristics.

It is clear from the experimental results shown in Fig. 1 that substantial shot-noise suppression occurs in the positive voltage resonant-tunneling regions. To see the amount of suppression quantitatively, we plot the shot-noise factor γ defined by $\gamma = i_n^2/(2eI)$ in Fig. 2.

To analyze the experimental results, we first use an analytical model to understand the basic physics involved. Numerical self-consistent calculations[13] taking into account the electron accumulation in the emitter and in the well and the electron depletion in the collector will be discussed in later sections. Theoretical analyses[7,8] under a variety of assumptions all give the following expression at zero temperature (with the exception of that of Brown[10] to be discussed later):

$$i_n^2 = 2e^2 A \sum_{E_F} v_z T(1-T), \tag{1}$$

where A is the device area, E_F is the Fermi energy in the emitter, v_z is the z-direction (tunneling direction) emitter electron velocity, T is the transmission coefficient defined as the ratio of the transmitted to incident probability currents, and the summation $\sum_{E_F}$ over the occupied emitter states for unit volume is the electron density. After converting the summation into an integration over the emitter Fermi sea and integrating over the parallel (x-y) momenta, Eq. (1) becomes

$$i_n^2 = 2e \frac{emA}{2\pi^2\hbar^3} \int_0^{E_F} dE\, T(1-T)(E_F - E), \tag{2}$$

where m is the effective mass and E is the electron energy associated with the z-direction motion. We have assumed that T is independent of the parallel momenta. Equations (1) and (2) take into account only the contribution from emitter electrons. This is a correct assumption for low temperatures and for bias voltages large enough so that the collector electrons do not contribute to the current. This is the regime (for bias voltage magnitudes larger than about 0.09 V) that we wish to concentrate on.

For evaluating the shot-noise factor, the tunneling current is given by[3]

$$I = \frac{emA}{2\pi^2\hbar^3} \int_0^{E_F} dE\, T(E_F - E). \tag{3}$$

In specifying the integration limits from zero to E_F in Eqs. (2) and (3) we have implicitly chosen the energy reference to be at the band edge of the emitter [see Fig. 3(a)].

In the resonant-tunneling regime, the transmission coefficient can be well approximated by a Breit-Wigner form[3]

$$T \approx T_{\max} \frac{\Delta E^2}{(E - E_r)^2 + \Delta E^2}, \tag{4}$$

where the on-resonance transmission is

$$T_{\max} = \frac{4T_1 T_2}{(T_1 + T_2)^2}, \tag{5}$$

ΔE is the resonance half-width, E_r is the resonance energy, and T_1 and T_2 are transmission coefficients for the two barriers labeled by 1 and 2.

Using Eq. (4), Eqs. (2) and (3) give

$$i_n^2 = 2e \Bigg\{ I - \frac{1}{2} \frac{emA}{2\pi^2\hbar^3} T_{\max}^2 \Delta E^2 \times \left[\frac{E_F - E_r}{\Delta E} \left(\arctan \frac{E_F - E_r}{\Delta E} + \arctan \frac{E_r}{\Delta E} \right) + \frac{\Delta E (E_F - E_r)}{(E_F - E_r)^2 + \Delta E^2} + \frac{\Delta E\, E_r}{E_r^2 + \Delta E^2} \right] \Bigg\}, \tag{6}$$

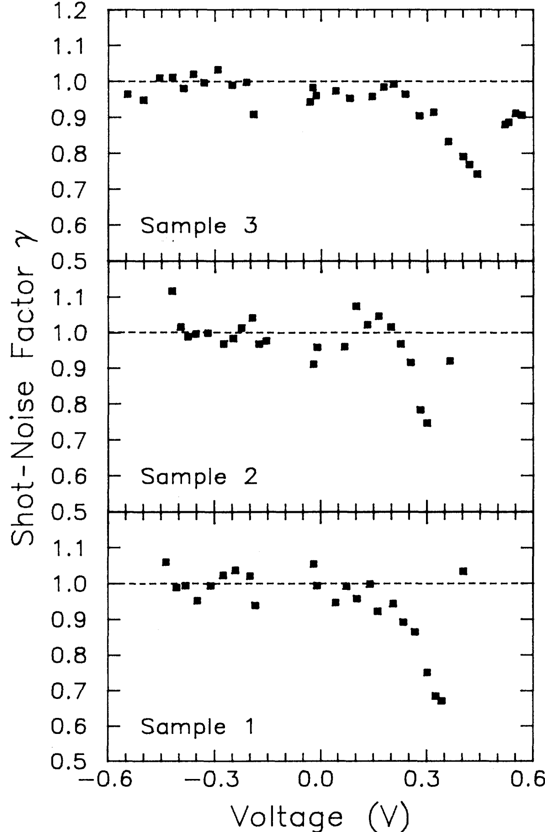

FIG. 2. Measured shot noise factor vs voltage at 4.2 K. The shot-noise factor γ is defined by $\gamma = i_n^2/2eI$, where i_n is the noise current in A/Hz$^{1/2}$ and I is the device current. A horizontal dashed line at $\gamma = 1$ is drawn to guide the eye.

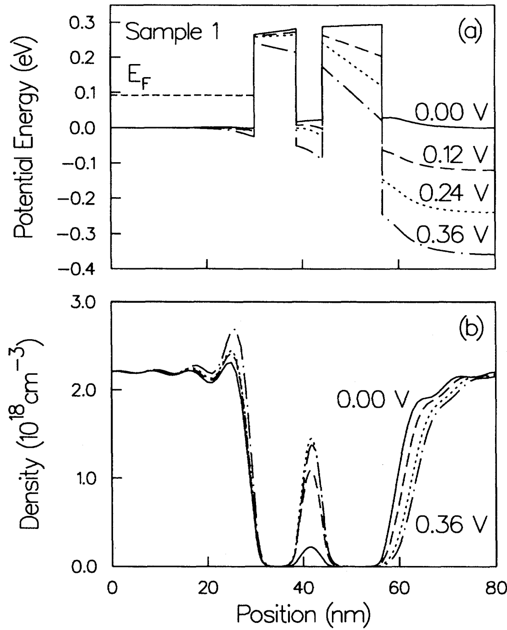

FIG. 3. (a) Calculated band edge and (b) electron density profile under a few positive bias voltage values for sample 1. For both panels (a) and (b), the solid curves are for an applied bias voltage of 0.00 V, the dashed for 0.12 V, the dotted for 0.24 V, and the chained for 0.36 V.

where I is given by

$$I = \frac{emA}{2\pi^2\hbar^3} T_{\max} \Delta E^2 \times \left[\frac{E_F - E_r}{\Delta E} \left(\arctan \frac{E_F - E_r}{\Delta E} + \arctan \frac{E_r}{\Delta E} \right) - \frac{1}{2} \ln \frac{(E_F - E_r)^2 + \Delta E^2}{E_r^2 + \Delta E^2} \right] . \quad (7)$$

Within the resonant-tunneling current region, $(E_F - E_r)/\Delta E \gg 1$ and $E_r/\Delta E \gg 1$ and the arctan terms in Eqs. (7) and (6) dominate. We then have $i_n^2 \approx 2e(1 - T_{\max}/2)I$. The shot-noise factor is then

$$\gamma = i_n^2/(2eI) \approx 1 - \frac{T_{\max}}{2}. \quad (8)$$

It is clear that a larger $T_{\max}$ value leads to a larger shot-noise suppression. However, the maximum value of $T_{\max}$ is unity, so the maximum shot-noise suppression occurs when $T_{\max} \to 1$ which gives $\gamma \to 1/2$. Achieving $T_{\max} \to 1$ is the basic aim of our sample design. Because of the finite bias voltage required to turn on the resonant tunneling, a symmetric double barrier under bias has the transmission coefficient for the emitter barrier much smaller than that for the collector barrier, and this [according to Eq. (5)] leads to a small $T_{\max}$. We therefore use different barriers with the collector barrier either thicker or higher than the emitter one so that, under appropriate bias voltages, the transmission coefficients for the emitter and the collector barriers are equal. This should yield a near unity $T_{\max}$ according to Eq. (5). Shot-noise suppression (i.e., $0.5 \leq \gamma < 1$), seen only in a finite region of positive bias, is in good qualitative agreement with the results shown in Figs. 1 and 2.

Although the basic approach of using an asymmetric double-barrier structure to achieve $T_{\max} \to 1$ is conceptually correct, the accurate prediction of the bias voltages at which $T_{\max} \to 1$ is nontrivial. The voltage drop across the double barrier is highly nonuniform due to charge buildup in the well, especially for asymmetric structures,[14] and the effect of electron accumulation in the emitter and depletion in the collector must be included in order to model accurately the voltage distribution across the structure. We therefore used a self-consistent program[13] using both Schrödinger and Poisson equations to calculate the device characteristics of our structures. The resulting band edge and electron density profiles for sample 1 are shown in Fig. 3. When the charge buildup in the well is large (as in the voltage range of 0.08–0.36 V), a larger fraction of the applied voltage is dropped across the collector barrier.

Figure 4 shows the results for the calculated transmission coefficients and the current-voltage and noise current characteristics, together with the measured results, for sample 1. The comparison of experimental and the-

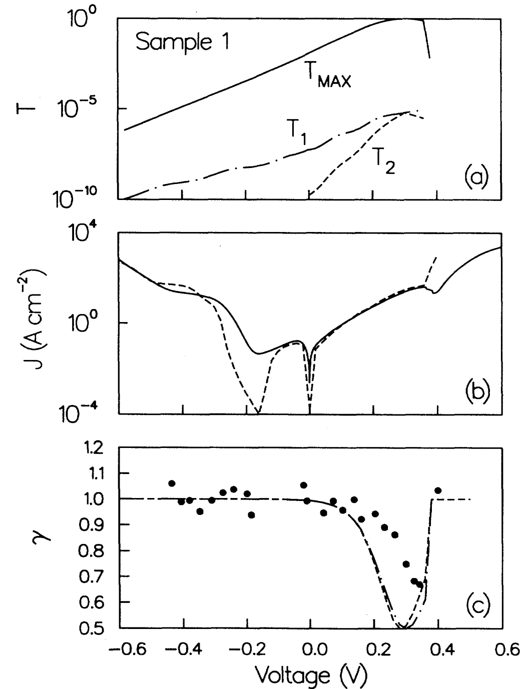

FIG. 4. (a) Calculated maximum transmission coefficient through the entire structure (solid curve), transmission through barrier 1 (chained curve), and barrier 2 (dashed curve), (b) calculated (dashed curve) and measured (solid curve) current density, and (c) calculated and measured shot-noise factor, all as a function of bias voltage for sample 1. In (c) the dashed curve is calculated from Eq. (8), the chained curve from Eq. (4.38) of Ref. 8, and the symbols show the measured values.

oretical current densities [Fig. 4(b)] shows two experimental features not reproduced accurately by the theory. These are the first negative differential resistance (NDR) regions seen above 0.36 V in positive bias and 0.14 V in negative bias. In both cases the failure of the theory is due to the neglect of scattering. In forward bias, the charge accumulation is very large, pushing the NDR region to much higher voltages. When the first resonant level drops below the emitter conduction band edge in the actual device, there is appreciable charge remaining in the well due to scattering to the resonant level from higher energies and the collector barrier does not drop sharply. The current is reduced as the resonant component switches off, leading to the NDR region. In contrast, the theoretical charge density in the well drops precipitously at this voltage and the resulting sharp redistribution in voltage drops leads to a huge increase in tunneling current. Under negative bias the theory underestimates the valley current due to nonresonant scattering contributions. Since the interesting shot-noise suppression occurs on resonance under positive bias, neither of these failures is critical to our analysis.

The calculated results shown in Fig. 4 quantitatively confirm several expectations from the simple analysis. In the voltage region around 0.3 V, $T_{\max}$ is nearly unity and correspondingly $T_1 \approx T_2$, consistent with Eq. (5). In the same voltage region and only in this region, $\gamma \to 0.5$ in agreement with Eq. (8). The experimental and the calculated shot-noise factors are in reasonably good agreement. However, the measured γ values are higher than the calculated ones in the voltage range of 0.2–0.36 V. This could be caused by some nonideal (for example, defect related) parallel conduction paths in addition to the ideal resonant-tunneling one, by the inaccuracy of the numerical model in predicting the voltage positions, or by the neglect of scattering noted above, which would reduce the $T_{\max}$ value below unity and lead to the observed results. Beyond this voltage region in the NDR region, no comparisons can be made because this region is not accessible by our experimental setup, and also because the numerical model breaks down.

We now discuss other related work in relation to the present work. This study was partly motivated by the work of Li *et al.*[11] The devices studied there also included asymmetric structures. However, they did not seem to see that the suppression had a strong voltage dependence for a given sample, whereas we find (as shown in Figs. 2 and 4) that only in the finite voltage range where the maximum transmission is close to unity is the shot noise significantly suppressed. To show the difference between our data and those of Li *et al.*, we plot the measured noise vs current, both normalized to $I_{\rm norm}$, in Fig. 5, where $I_{\rm norm}$ is the current at the resonant peak for positive bias. The inset shows the negative voltage data normalized to the current at the resonant peak for negative bias in order to expand the low current region for this bias. If Fig. 5 is compared with Fig. 3 of Li *et al.*, significant differences can be seen: for example, their sample $S2$ showed only a small amount of suppression under forward bias, and $S3$ showed suppression of the same magnitude as ours but for *both* forward and reverse

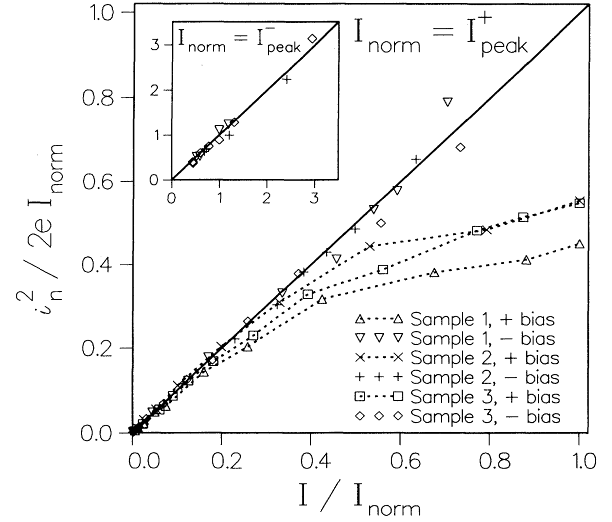

FIG. 5. Normalized noise vs current. $I_{\rm norm}$ is the current at the resonant peak of positive bias. The inset shows the negative voltage data normalized to the current at the resonant peak of negative bias.

bias voltages and apparently independent of the current. Furthermore, Li *et al.* qualitatively discussed their observed shot noise suppression in terms of incoherent and sequential tunneling, implying that for coherent tunneling a full shot noise ($\gamma = 1$) is expected. The expectation of $\gamma = 1/2$ for fully sequential tunneling may be justified; but coherence does not imply that γ is equal to 1—as shown, for example, by Büttiker,[7] Beenakker and Büttiker,[15] and by Eq. (8).

Our work was also partly motivated by the prediction by Brown[10] and by van de Roer *et al.*[12] of a feedback effect due to the charge buildup, giving rise to a shot-noise suppression. The basic idea is that since the current and the built-up charge are directly related, a fluctuation in the current leads to a fluctuation in the built-up charge which in turn modifies the potential, resulting in a change in current. The devices studied by Brown and by van de Roer *et al.* were symmetric ones for which a smaller amount of charge buildup is expected. We therefore designed the asymmetric samples to enhance the effect. In addition, if this feedback effect *did* cause a reduction in the shot noise, we would observe the suppression not only in the region where $T_{\max} \to 1$ but also in the region where transmission through the emitter barrier is much higher than that for the collector barrier, because in this region the charge buildup in the well is maximal.[3,14] From Fig. 3(b), there is a substantial amount of charge buildup for all nonzero positive voltages, and from Fig. 4(a), $T_1 \gg T_2$ for all positive voltages up to about 0.3 V; however, suppression is only seen in a smaller range of voltages. Our experiments therefore do not provide any additional evidence of the effect proposed by Brown[10] and by van de Roer *et al.*[12] although we cannot rule out its existence due to the limited accuracy of the calculated results in comparison with experiments as shown in Fig. 4(c).

In our discussion throughout Eqs. (1)–(8), we have used a completely coherent approach neglecting any scattering effects. While this may be justified for phase-preserving elastic scattering perturbations if an appropriate broadening in the resonance width is included for Eq. (4), the effects of dephasing and dissipation must be considered since the intrinsic characteristic time scales for our structures are not very short by comparison with scattering times. However, this is a complicated issue that deserves further study.[9,15] The use of results derived from a coherent approach is consistent with the theoretical results of Shimizu and Ueda.[9] A central result of theirs is that Eq. (1) formally holds even when the phase is destroyed during the traversal of an electron through the structure. They concluded, however, that dissipation would cause a modification of Eq. (1). Since optical phonon scattering is the dominant energy relaxation process here and since our results are identical for temperatures of 4.2 and 77 K, dissipation may be neglected here.

In summary, we have shown that the shot noise is suppressed in resonant tunneling *only* when the transmission is large, and that the maximum shot-noise suppression is given by a factor approaching 1/2 when the transmission is near unity. This suppression is expected to be found in other nanostructures with high transmission coefficients.

We have benefited from discussions with G. Iannaccone.

---

* FAX: 613 957 8734. Electronic address: H.C.LIU@NRC.CA

[1] L. L. Chang, L. Esaki, and R. Tsu, Appl. Phys. Lett. **24**, 593 (1974).

[2] E. R. Brown, in *Hot Carriers in Semiconductor Nanostructures*, edited by J. Shah (Academic Press, Boston, 1992), pp. 469–498.

[3] H. C. Liu and T. C. L. G. Sollner, in *High-Speed Heterostructure Devices*, edited by R. A. Kiehl and T. C. L. G. Sollner, Semiconductors and Semimetals Vol. 41 (Academic Press, San Diego, 1994), Chap. 6, pp. 359–419.

[4] R. K. Hayden, D. K. Maude, L. Eaves, E. C. Valadares, M. Henini, F. W. Sheard, O. H. Hughes, J. C. Portal, and L. Cury, Phys. Rev. Lett. **66**, 1749 (1991).

[5] H. C. Liu, M. Buchanan, G. C. Aers, Z. R. Wasilewski, T. W. Moore, R. L. S. Devine, and D. Landheer, Phys. Rev. B **43**, 7086 (1991).

[6] L. Y. Chen and C. S. Ting, Phys. Rev. B **43**, 4534 (1991).

[7] M. Büttiker, Phys. Rev. B **46**, 12 485 (1992).

[8] J. H. Davies, P. Hyldgaard, S. Hershfield, and J. W. Wilkins, Phys. Rev. B **46**, 9620 (1992).

[9] A. Shimizu and M. Ueda, Phys. Rev. Lett. **69**, 1403 (1992).

[10] E. R. Brown, IEEE Trans. Electron Devices **39**, 2686 (1992).

[11] Y. P. Li, A. Zaslasky, D. C. Tsui, M. Santos, and M. Shayegan, Phys. Rev. B **41**, 8388 (1990).

[12] T. G. van de Roer, H. C. Heyker, J. J. M. Kwaspen, H. P. Joosten, and M. Henini, Electron. Lett. **27**, 2158 (1991).

[13] D. Landheer and G. C. Aers, Superlatt. Microstruct. **7**, 17 (1990).

[14] H. C. Liu, G. C. Aers, M. Buchanan, Z. R. Wasilewski, and D. Landheer, J. Appl. Phys. **70**, 935 (1991).

[15] C. W. J. Beenakker and M. Büttiker, Phys. Rev. B **46**, 1889 (1992).